

# Thyroid hormones induce browning of white fat

Noelia Martínez-Sánchez<sup>1,2</sup>, José M Moreno-Navarrete<sup>2,3</sup>, Cristina Contreras<sup>1,2</sup>,  
Eva Rial-Pensado<sup>1,2</sup>, Johan Fernø<sup>1,4</sup>, Rubén Nogueiras<sup>1,2</sup>, Carlos Diéguez<sup>1,2</sup>,  
José-Manuel Fernández-Real<sup>2,3</sup> and Miguel López<sup>1,2</sup>

<sup>1</sup>Department of Physiology, CIMUS, University of Santiago de Compostela-Instituto de Investigación Sanitaria, Santiago de Compostela, Spain

<sup>2</sup>CIBER Fisiopatología de la Obesidad y Nutrición (CIBEROBN), Santiago de Compostela, Spain

<sup>3</sup>Department of Diabetes, Endocrinology and Nutrition, Hospital de Girona 'Dr Josep Trueta', Institut D'investigació Biomèdica de Girona (IdIBGi) and University of Girona, Girona, Spain

<sup>4</sup>Department of Clinical Science, KG Jebsen Center for Diabetes Research, University of Bergen, Bergen, Norway

Correspondence  
should be addressed  
to J-M Fernández-Real or  
Miguel López  
**Email**  
jmfreal@idibgi.org or  
m.lopez@usc.es

## Abstract

The canonical view about the effect of thyroid hormones (THs) on thermogenesis assumes that the hypothalamus acts merely as a modulator of the sympathetic outflow on brown adipose tissue (BAT). Recent data have challenged that vision by demonstrating that THs act on the ventromedial nucleus of the hypothalamus (VMH) to inhibit AMP-activated protein kinase (AMPK), which regulates the thermogenic program in BAT, leading to increased thermogenesis and weight loss. Current data have shown that in addition to activation of brown fat, the browning of white adipose tissue (WAT) might also be an important thermogenic mechanism. However, the possible central effects of THs on the browning of white fat remain unclear. Here, we show that 3,3',5,5' tetraiodothyroxene (T<sub>4</sub>)-induced hyperthyroidism promotes a marked browning of WAT. Of note, central or VMH-specific administration of 3,3',5-triiodothyronine (T<sub>3</sub>) recapitulates that effect. The specific genetic activation of hypothalamic AMPK in the VMH reversed the central effect of T<sub>3</sub> on browning. Finally, we also showed that the expression of browning genes in human WAT correlates with serum T<sub>4</sub>. Overall, these data indicate that THs induce browning of WAT and that this mechanism is mediated via the central effects of THs on energy balance.

## Key Words

- ▶ AMPK
- ▶ browning
- ▶ thyroid hormones
- ▶ white adipose tissue

*Journal of Endocrinology*  
(2017) **232**, 351–362

## Introduction

Thyroid hormones (THs; 3,3',5,5' tetraiodothyroxene or T<sub>4</sub> and 3,3',5-triiodothyronine or T<sub>3</sub>) exert important biological actions, not only modulating the development and growth but also regulating metabolism and energy balance (Brent 2012, Warner & Mittag 2012, Lopez *et al.* 2013). Impaired function of the thyroid gland, by either hyperthyroidism or hypothyroidism, leads to alterations in metabolism and energy homeostasis. Hyperthyroidism is associated with an increase in the metabolic rate and the patients suffering from this condition undergo body

weight loss, despite increased food intake; quite the opposite, hypothyroid patients show lowered metabolic rate and reduced food intake (Brenta *et al.* 2007, Kaptein *et al.* 2009, Pearce 2012).

THs are key regulators of thermogenesis, which represents a major component of the energy expenditure in homeothermic ('warm-blooded') animals (Cannon & Nedergaard 2004, Silva 2006). In mammals, including humans, thermogenesis occurs mainly in the brown adipose tissue (BAT) (Cannon & Nedergaard 2004,

Silva 2006, von Ballmoos *et al.* 2009). THs act on brown adipocyte thermogenesis by increasing the stimulatory action of norepinephrine (NE), as well as enhancing the cAMP-mediated acute rise in *ucp1* gene expression (Bianco *et al.* 1988, Silva 2006, Ribeiro *et al.* 2010). The existence of central effects of THs in the regulation of BAT thermogenesis was proposed long time ago (Nedergaard *et al.* 1997). Recent evidence from our group has also shown a homeostatic link between the central effects of THs on hypothalamic AMP-activated protein kinase (AMPK), sympathetic tone and UCP1 expression in BAT (Lopez *et al.* 2010, Alvarez-Crespo *et al.* 2016).

Over the last years, accumulating evidence has demonstrated that activation of beige/brite ('brown in white') adipocytes in the white adipose tissue (WAT), a process known as browning (Fisher *et al.* 2012, Cohen *et al.* 2014, Nedergaard & Cannon 2014, Contreras *et al.* 2016b), is responsible for a significant increase in total energy expenditure (Shabalina *et al.* 2013). Thus, stimulation of browning has therapeutic potential to promote body fat reduction (Yoneshiro *et al.* 2013, Beiroa *et al.* 2014). Several mechanisms have been proposed for WAT browning (Villarroya & Vidal-Puig 2013, Nedergaard & Cannon 2014), including prolonged cold exposure (Loncar *et al.* 1986), adrenergic activation (Cousin *et al.* 1992, Ghorbani *et al.* 1997, Cao *et al.* 2011) and also thyroid hormone receptor (TR) agonism (Lin *et al.* 2015, Alvarez-Crespo *et al.* 2016). However, the role of central THs in the control of WAT browning remains unclear.

The aim of this study was to investigate the role of central THs on the browning of WAT and the mechanisms behind this action. Our data show that peripherally induced hyperthyroidism promoted browning of white fat and that this effect is recapitulated by central and specific administration of T<sub>3</sub> in the ventromedial nucleus of hypothalamus (VMH), via a mechanism dependent of AMPK. Notably, we also demonstrate that the expression of browning markers in WAT correlates with serum T<sub>4</sub> levels in humans. Thus, in addition to the well-known effects of central THs on BAT (Lopez *et al.* 2010, Alvarez-Crespo *et al.* 2016), our data indicate an additional mechanism by which central THs influence energy expenditure, namely browning of WAT.

## Material and methods

### Animals

Male Sprague–Dawley rats (200–250g; Animalario General USC, Santiago de Compostela, Spain) were housed

on a 12-h light (08:00–20:00), 12-h darkness cycle, in a temperature and humidity controlled room and maintained with chow (STD, SAFE A04: 3.1% fat, 59.9% carbohydrates, 16.1% proteins, 2.791kcal/g; Scientific Animal Food & Engineering; Nantes, France) and water *ad libitum*. For all the procedures, the animals were individually caged and used for experimentation 7 days later. During all experimental approaches, animals and their respective food intake and body weight were monitored every day. The experiments were performed in agreement with the International Law on Animal Experimentation and were approved by the USC Ethical Committee (Project ID 15010/14/006).

### Patients

A group of 163 (80 visceral, vWAT and 83 subcutaneous, sWAT) white adipose tissues from participants were analyzed (Table 1). These participants were recruited at the Endocrinology Service of the Hospital of Girona 'Dr Josep Trueta'. All subjects were of Caucasian origin and reported that their body weight had been stable for at least three months before the study. Subjects were studied in their post-absorptive state. They had no systemic disease other than obesity and all were free of any infections in the previous month before the study. Liver diseases (specifically tumoral disease and HCV infection) and thyroid dysfunction were exclusion criteria. All subjects gave written informed consent, validated and approved by the Ethics committee of the Hospital of Girona 'Dr Josep Trueta', after the purpose of the study was explained to them.

### Induction of hyperthyroidism

Hyperthyroidism in rats was induced by chronic subcutaneous (SC) administration of L-thyroxine

**Table 1** Anthropometric and clinical parameters.

|                                   |                    |
|-----------------------------------|--------------------|
| Sex (men/women) <sup>†</sup>      | 14/69              |
| Age (years)                       | 45.24 ± 10.5       |
| BMI (kg/m <sup>2</sup> )          | 42.3 ± 8.4         |
| Fasting glucose (mg/dL)           | 95.5 (85.5–112.2)* |
| Total cholesterol (mg/dL)         | 186.3 ± 30.3       |
| HDL cholesterol (mg/dL)           | 55.1 ± 16.5        |
| LDL cholesterol (mg/dL)           | 108.9 ± 28.7       |
| Fasting triglycerides (mg/dL)     | 102 (79–145)*      |
| Serum free T <sub>4</sub> (ng/dL) | 1.21 ± 0.18        |

Mean ± s.d. for normal distributed variables.

\*Median (interquartile range) for non-normal distributed variables. †Qualitative variables are expressed as frequencies.

(T<sub>4</sub>, 100 µg/day, dissolved in 200 µL of saline; Sigma) for a period of three weeks (21 days), as previously described (Lopez *et al.* 2010, Gonzalez *et al.* 2012, Varela *et al.* 2012). Euthyroid (control) rats were treated with vehicle (saline).

### Intracerebroventricular treatments

Intracerebroventricular (ICV) cannulas were stereotaxically implanted under ketamine/xylazine anesthesia, as previously described (Lopez *et al.* 2008, 2010, Whittle *et al.* 2012, Contreras *et al.* 2014, Martinez de Morentin *et al.* 2014, Alvarez-Crespo *et al.* 2016, Martins *et al.* 2016), using the following coordinates 1.6 mm lateral to bregma, 0.6 mm posterior, 4.5 mm deep from the skull. Rats received a single ICV daily administration of T<sub>3</sub> (4 ng/day, during 5 days) dissolved in 5 µL of saline.

### Stereotaxic microinjection of T<sub>3</sub> and viral vectors

Rats were placed in a stereotaxic frame (David Kopf Instruments; Tujunga, CA, USA) under ketamine/xylazine anesthesia. Nuclei-specific injections were delivered via a permanent 28-gauge stainless steel cannula (Plastics One, Roanoke, VA, USA) inserted bilaterally either in the VMH or the arcuate nucleus of the hypothalamus (ARC), following stereotaxic coordinates: (a) for the VMH: -2.8 mm posterior to the bregma, ±0.6 mm lateral to bregma and 10.1 mm deep from the skull; (b) for the ARC: -2.8 mm posterior to the bregma, ±0.3 mm lateral to bregma and 10.2 mm deep from the skull. A catheter tube was connected from each infusion cannula to an osmotic minipump flow moderator (Model 1007D; Alzet Osmotic Pumps, Cupertino, CA, USA). These pumps had a flow rate of 0.5 µL/h during 7 days of treatment. The osmotic minipumps were inserted in a subcutaneous pocket on the dorsal surface created using blunt dissection (Imbernon *et al.* 2013, Contreras *et al.* 2014, Martins *et al.* 2016).

Adenoviral GFP or constitutive active AMPK $\alpha$  isoforms (AMPK $\alpha$ -CA; Viraquest; North Liberty, IA, USA) vectors (Woods *et al.* 2000, Minokoshi *et al.* 2004, Lopez *et al.* 2008, 2010) were delivered in the VMH of rats using a 25-gauge needle (Hamilton; Reno, NV, USA) and the stereotaxic coordinates: -2.4 mm and -3.2 mm posterior to the bregma, ±0.6 mm lateral to bregma and 10.1 mm deep at a rate of 200 nL/min for 5 min for rat (1 µL/injection site) as previously reported (Lopez *et al.* 2008, 2010, Martinez de Morentin *et al.* 2012, 2014, Whittle *et al.* 2012, Beiroa *et al.* 2014, Contreras *et al.* 2014, Martins *et al.* 2016). Animals were treated for 6 days.

### Blood biochemistry

For the rat samples, plasma levels of T<sub>3</sub> and T<sub>4</sub> were measured using rat ELISA kits (Crystal Chem Inc; Downers Grove, IL, USA) (Lopez *et al.* 2010, Gonzalez *et al.* 2012, Varela *et al.* 2012). For the human samples, serum glucose concentrations were measured in duplicate by the glucose oxidase method using a Beckman Glucose Analyser II (Beckman Instruments; Brea, CA, USA). Roche Hitachi Cobas c711 instrument (Roche) was used to perform HDL cholesterol and total serum triglycerides determinations. HDL cholesterol was quantified by a homogeneous enzymatic colorimetric assay through the cholesterol esterase/cholesterol oxidase/peroxidase reaction (Cobas HDLC3; Roche). Serum fasting triglycerides were measured by an enzymatic, colorimetric method with glycerol phosphate oxidase and peroxidase (Cobas TRIGL; Roche). LDL cholesterol was calculated using the Friedewald formula. Serum free T<sub>4</sub> was measured by electrochemiluminescence (Roche Diagnostics) with intra- and inter-assay coefficients of variation less than 5%. Methods have been previously reported (Ortega *et al.* 2015, Gavalda-Navarro *et al.* 2016).

### Sample processing

Rats were killed by cervical dislocation. From each animal, gonadal WAT (gWAT), subcutaneous inguinal WAT (sWAT) or both (only for the euthyroid and hyperthyroid animals) were harvested and immediately frozen in dry ice. Samples were stored at -80°C until further processing. Human adipose tissue samples were obtained from sWAT and vWAT depots during elective surgical procedures (cholecystectomy, surgery of abdominal hernia and gastric bypass surgery) (Ortega *et al.* 2015, Gavalda-Navarro *et al.* 2016). Samples of adipose tissue were immediately transported to the laboratory (5–10 min). Tissue handling was carried out under strictly aseptic conditions. Adipose tissue samples were washed in PBS, cut off with forceps and scalpel into small pieces (100 mg), and immediately flash-frozen in liquid nitrogen before storage at -80°C.

### Real-time PCR

We performed real-time PCR (TaqMan; Applied Biosystems) as previously described (Lopez *et al.* 2010, Martinez de Morentin *et al.* 2012, 2014, Whittle *et al.* 2012, Contreras *et al.* 2014, Alvarez-Crespo *et al.* 2016, Martins *et al.* 2016), using specific sets of primers and probes for rat (Supplementary Table 1, see section on

supplementary data given at the end of this article). Values were expressed relative to hypoxanthine–guanine phosphoribosyltransferase (HPRT) levels. For the analysis of the human WAT samples, we used commercially available and pre-validated TaqMan primer/probe sets (Applied Biosystems) as follows: endogenous control peptidylprolyl isomerase A (cyclophilin A) (*PPIA*, 4333763), PR domain containing 16 (*PRDM16*, Hs00223161\_m1), uncoupling protein 1 (*UCP1*, Hs00222453\_m1) and cell death-inducing DFFA-like effector a (*CIDEA*, Hs00154455\_m1). Gene expression values were expressed relative to *PPIA* levels.

### Histology and immunohistochemistry

Adipose tissue depots were fixed in 10% buffered formaldehyde. For the hematoxylin–eosin processing, the WAT sections were first stained with hematoxylin for 5 min, washed and stained again with eosin for 1 min. The detection of UCP1 in WAT was performed using anti-UCP1 (1:500; ab10983; Abcam) as previously reported (Alvarez-Crespo *et al.* 2016, Martins *et al.* 2016). The specificity of the UCP1 antibody has been previously validated by using WAT samples from UCP1 KO mice (Alvarez-Crespo *et al.* 2016). Images were taken with a digital camera Olympus XC50 (Olympus Corporation) at 20 $\times$ . Digital images from WAT for immunohistochemistry were quantified with FRIDA image analysis software (FRIDA Software; The Johns Hopkins University; MD, USA); briefly, a color mask (pixel threshold masks) was set to define the UCP1 staining. This color mask was applied to all photographs, and the software obtained a numeric value proportional to the color level in each image. These values are represented with respect to control (100%). For the adipocyte area, images were analyzed with ImageJ Software (National Institutes of Health; MD, USA). Direct detection of GFP fluorescence was performed after perfusion of the animals and detected with a fluorescence microscope Olympus IX51, at 4 $\times$ .

### Statistical analysis

For the rat experiments, data are expressed as mean  $\pm$  s.e.m. (error bars represent s.e.m.), mRNA and protein data were expressed in relation (%) to control (euthyroid, vehicle-treated or GFP) rats. Statistical significance was determined by Student's *t*-test when two groups were compared or ANOVA followed by two-tailed Bonferroni *post hoc* test when more than two groups were compared.  $P < 0.05$  was

considered statistically significant. For the human studies, statistical analyses were performed using SPSS 12.0 software (IBM). Descriptive results of continuous variables are expressed as mean and s.d. for Gaussian variables or median and interquartile range unless otherwise stated. Parameters that did not fulfill normal distribution were mathematically Log transformed to improve symmetry for subsequent analyses. The relation between variables was analyzed by simple correlation (Pearson's test and Spearman's test) and by multivariate regression analysis. Levels of statistical significance were set at  $P < 0.05$ .

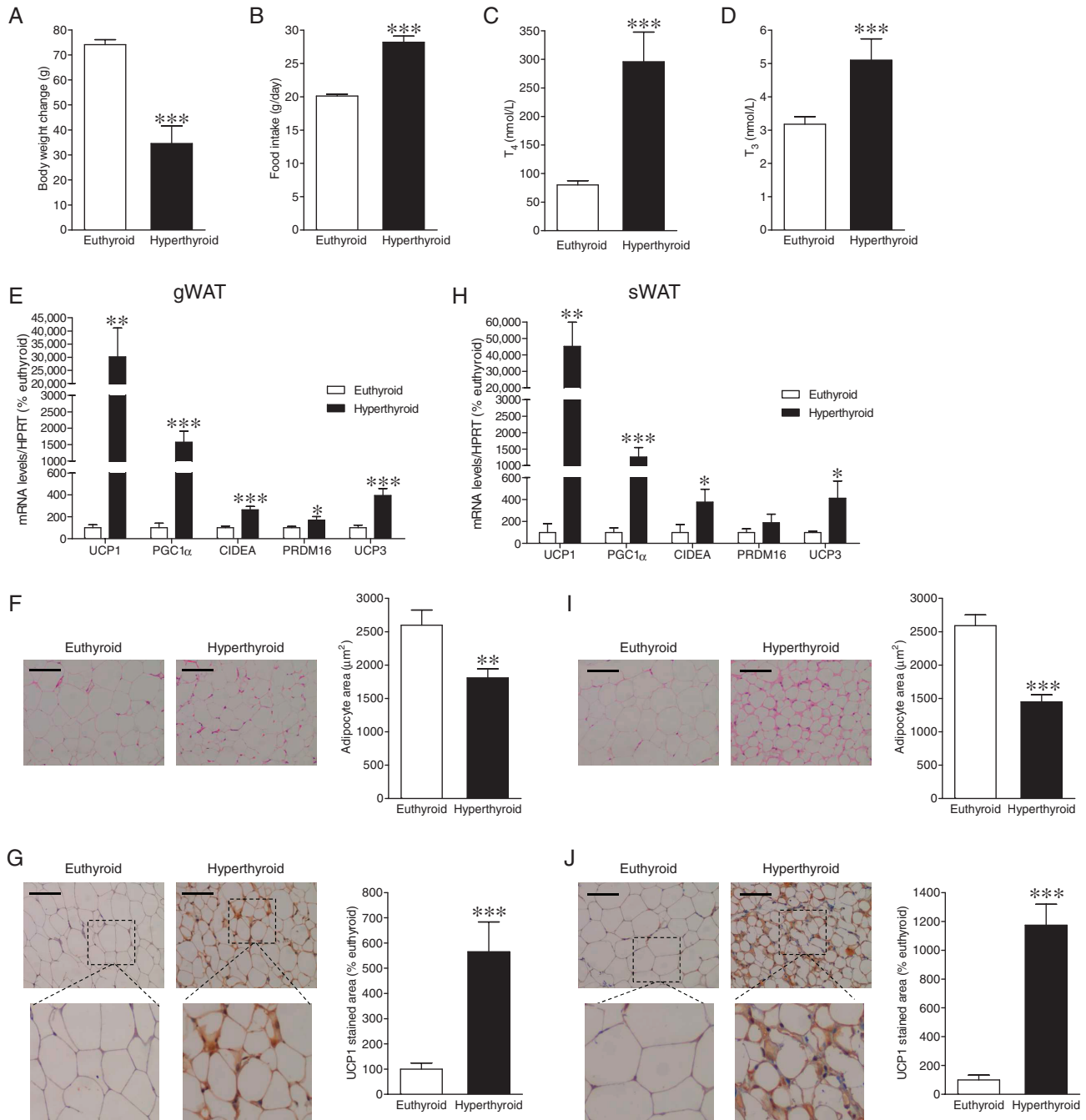
## Results

### Hyperthyroidism induces browning of WAT in rats

$T_4$ -treated rats exhibited decreased weight gain (Fig. 1A) despite hyperphagia (Fig. 1B). Increased circulating levels of  $T_4$  (Fig. 1C) and  $T_3$  (Fig. 1D), confirmed their hyperthyroid status. Next, we analyzed whether hyperthyroidism induced browning of WAT in these animals. Our mRNA data showed that the mRNA expression of browning markers, such as UCP1, peroxisome proliferator-activated receptor gamma coactivator 1-alpha (*PGC1 $\alpha$* ), *CIDEA*, *PRDM16* and also of uncoupling protein 3 (*UCP3*) was significantly increased in the gWAT (Fig. 1E) and sWAT (Fig. 1H) of hyperthyroid rats. Histological analysis of WAT showed that hyperthyroid rats exhibited a 'brown-like' multilocular pattern, associated with decreased adipocyte area (Fig. 1F and I) and increased UCP1 immunostaining (Fig. 1G and J) in both gWAT and sWAT.

### Central $T_3$ induces browning of WAT in rats

Recent data have shown that the effect of THs on thermogenesis is centrally mediated (Lopez *et al.* 2010, Alvarez-Crespo *et al.* 2016). Therefore, we hypothesized that central chronic exposure of  $T_3$  may stimulate browning of WAT. ICV  $T_3$  administration induced a feeding-independent decrease in body weight (Fig. 2A and B). mRNA analysis of gWAT showed tendencies even though statistically non-significant for browning markers to be increased (Fig. 2C). Nevertheless, and more relevant, when histological analyses were assessed, our results were much clearer, indicating that ICV  $T_3$ -treated rats displayed a 'brown-like' multilocular pattern, associated to decreased adipocyte area (Fig. 2D) and increased UCP1 immunostaining (Fig. 2E).

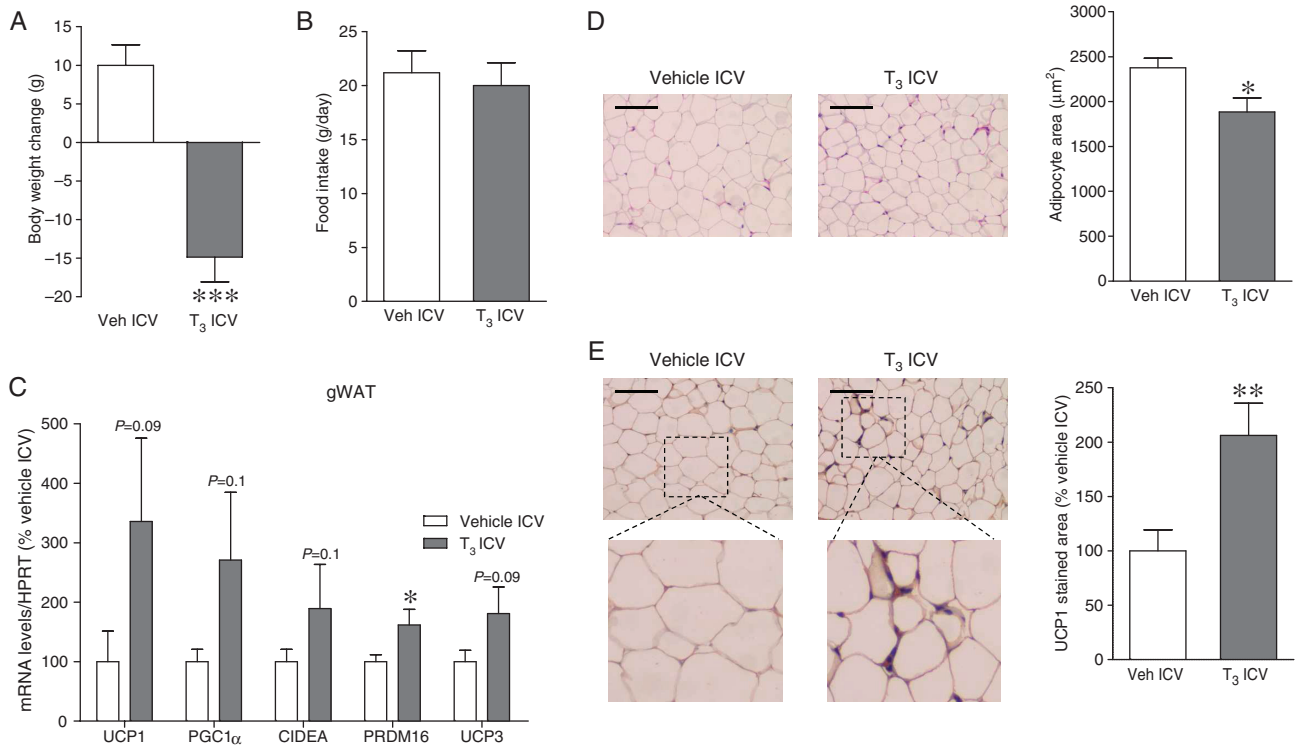
**Figure 1**

Effect of hyperthyroidism on WAT browning. (A) Body weight change, (B) daily food intake, (C) T<sub>4</sub> and (D) T<sub>3</sub> circulating levels of euthyroid and hyperthyroid rats. (E and H) mRNA expression of browning markers, (F and I) representative H&E staining (left panels; 20 $\times$ , scale bar: 100  $\mu$ m) and adipocyte area (right panels), and (G and J) representative immunohistochemistry with anti-UCP1 antibody showing UCP1 staining (left panels; 20 $\times$ , scale bar: 100  $\mu$ m), UCP1 stained area (right panels) in gWAT and sWAT of euthyroid and hyperthyroid rats. Statistical significance was determined by Student's *t*-test. *N* = 7 (only for the IHC analyses)-10 animals per group. Error bars represent s.e.m. \*, \*\* and \*\*\**P* < 0.05, 0.01 and 0.001 vs euthyroid.

### T<sub>3</sub> in the VMH, but not in the ARC, induces browning of WAT in rats

Next, we aimed to identify the hypothalamic nucleus where T<sub>3</sub> exerted its action on WAT. Therefore, we

performed chronic stereotaxic administration of T<sub>3</sub> into the VMH and the neighboring ARC. The correct position of the cannulae was verified by histological examination of coronal sections of the

**Figure 2**

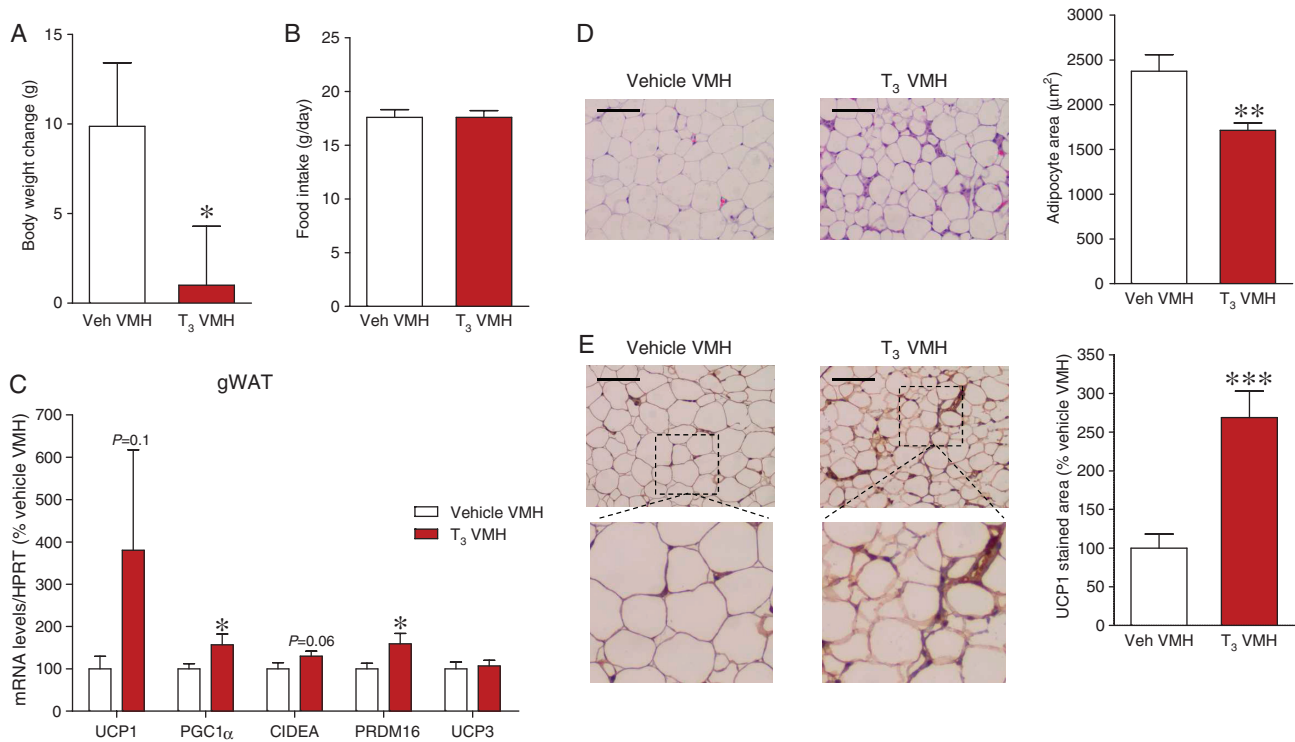
Effect of central T<sub>3</sub> administration on WAT browning. (A) Body weight change, (B) daily food intake, (C) mRNA expression of browning markers (D) representative H&E staining (left panels; 20 $\times$ , scale bar: 100  $\mu\text{m}$ ) and adipocyte area (right panels), and (E) representative immunohistochemistry with anti-UCP1 antibody showing UCP1 staining (left panels; 20 $\times$ , scale bar: 100  $\mu\text{m}$ ), UCP1 stained area (right panels) in gWAT of vehicle- or T<sub>3</sub> ICV-treated rats. Statistical significance was determined by Student's *t*-test. *N*=7 (only for the IHC analyses)-14 animals per group. Error bars represent s.e.m. \**P*<0.05, \*\**P*<0.01, \*\*\**P*<0.001 vs vehicle.

brains (data not shown). When given into the VMH, T<sub>3</sub> promoted a feeding-independent weight loss (Fig. 3A and B). On the other hand, when T<sub>3</sub> was administered into the ARC, there was a tendency to increase body weight at the end of the treatment, which was associated with hyperphagia (Supplementary Fig. 1A and B). mRNA analysis of gWAT showed significantly increased or clear trends toward increased levels of browning markers when T<sub>3</sub> was delivered within the VMH (Fig. 3C), but not the ARC (Supplementary Fig. 1C). Again, histological analyses confirmed that VMH T<sub>3</sub>-treated rats displayed decreased adipocyte area (Fig. 3D) and increased UCP1 immunostaining (Fig. 3E) in gWAT, confirming browning.

### Central effects of T<sub>3</sub> on browning of WAT depend on AMPK in the VMH

Next, we investigated the molecular mechanisms within the VMH leading to modulation of browning after central T<sub>3</sub> administration. Recent evidence has linked the inhibition of hypothalamic AMPK, and more specifically within the VMH, as a mechanism for the central regulation of BAT

thermogenesis by THs (Lopez *et al.* 2010, 2016, Alvarez-Crespo *et al.* 2016). Based on this evidence, we hypothesized that the central effect of T<sub>3</sub> on browning might be mediated by specific inhibition of AMPK in the VMH. To test this, adenoviruses encoding either a constitutively active isoform of AMPK $\alpha$  (AMPK $\alpha$ -CA) or a GFP control vector were injected stereotaxically into the VMH of ICV T<sub>3</sub>-treated rats. The AMPK $\alpha$ -CA adenovirus was previously validated (Lopez *et al.* 2010, Martinez de Morentin *et al.* 2012, 2014, Whittle *et al.* 2012, Beiroa *et al.* 2014, Martins *et al.* 2016). Overexpression of AMPK $\alpha$ -CA in the VMH, confirmed by GFP immunofluorescence (Fig. 4A), blunted the weight loss caused by central T<sub>3</sub> injection, without alteration in feeding (Fig. 4B and C). Of note, this effect was associated with the reversal of the T<sub>3</sub>-induced browning of gWAT, as demonstrated by increased adipocyte area (Fig. 4D) and decreased UCP1 staining (Fig. 4E) in T<sub>3</sub>-treated rats receiving AMPK $\alpha$ -CA adenoviruses in the VMH compared with those treated with control GFP adenoviruses. Together, these results are consistent with the observation that AMPK activity in the VMH mediates the central effects of T<sub>3</sub> on browning of WAT.

**Figure 3**

Effect of  $T_3$  in the VMH on WAT browning. (A) Body weight change, (B) daily food intake, (C) mRNA expression of browning markers, (D) representative H&E staining (left panels; 20 $\times$ , scale bar: 100  $\mu$ m) and adipocyte area (right panels), and (E) representative immunohistochemistry with anti-UCP1 antibody showing UCP1 staining (left panels; 20 $\times$ , scale bar: 100  $\mu$ m), UCP1 stained area (right panels) in gWAT of vehicle- or  $T_3$ -treated rats in the VMH. Statistical significance was determined by Student's *t*-test.  $N=7$  (only for the IHC analyses)-18 animals per group. Error bars represent s.e.m. \*, \*\* and \*\*\* $P<0.05$ , 0.01 and 0.001 vs vehicle.

### Browning markers in WAT are positively correlated with circulating $T_4$ in humans

Finally, we analyzed the relationship between  $T_4$  serum concentrations and the mRNA expression levels of browning marker in sWAT and vWAT, in samples derived from a large cohort of patients. Our data showed that the mRNA levels of UCP1 and CIDEA in sWAT (Fig. 5A and B, Supplementary Fig. 2) and PRDM16 in sWAT and vWAT (Fig. 5C and D), correlated with circulating free  $T_4$ , showing a positive association between THs and browning in humans. Multivariate regression analysis indicated that serum free  $T_4$  levels contributed significantly to browning-related (PRDM16, CIDEA and UCP1) mRNA levels variation after controlling for age, gender and BMI (Table 2).

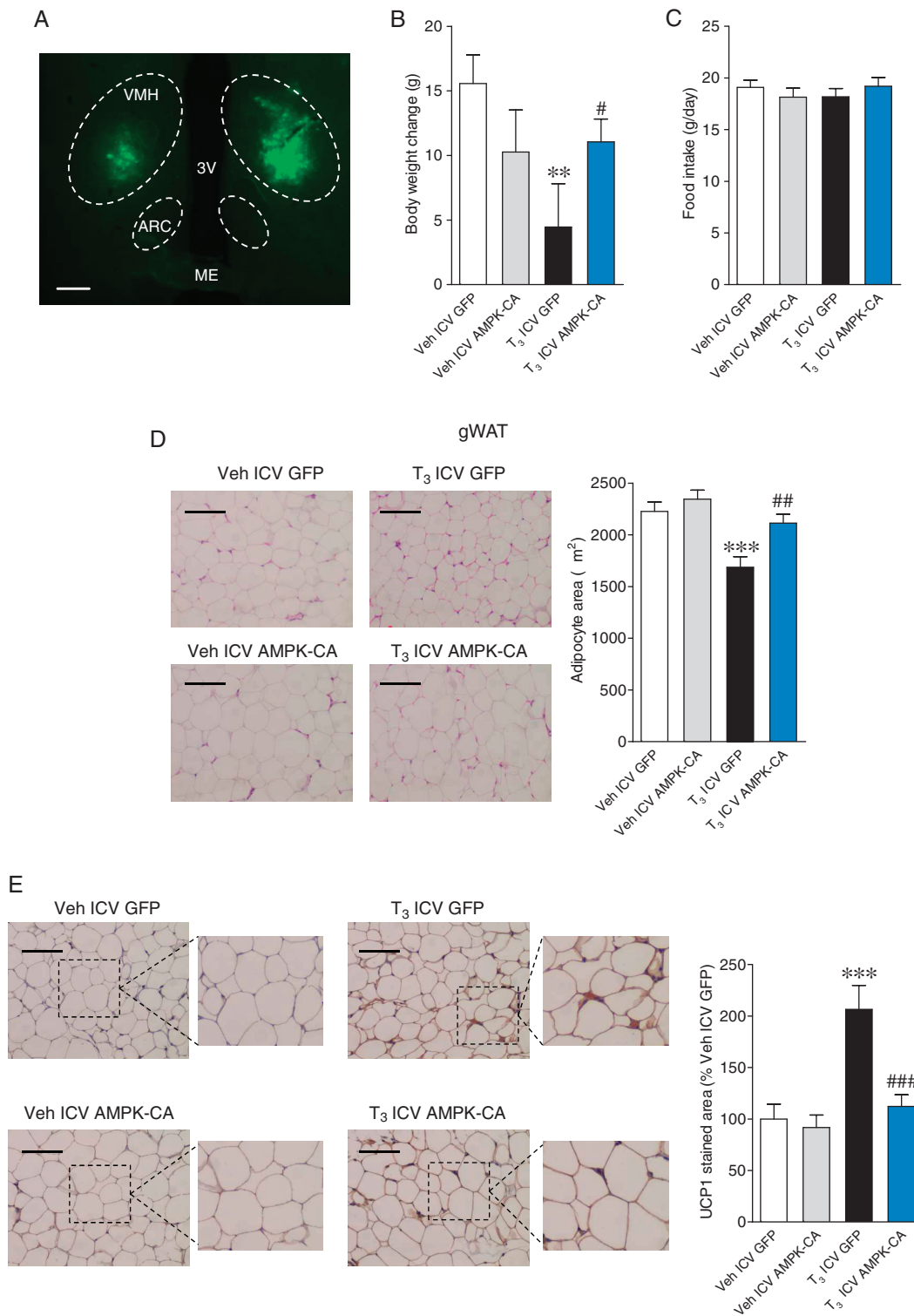
## Discussion

In this study, we show that THs induce browning of WAT in rodents and circulating  $T_4$  levels correlate with the expression of browning markers in the WAT of

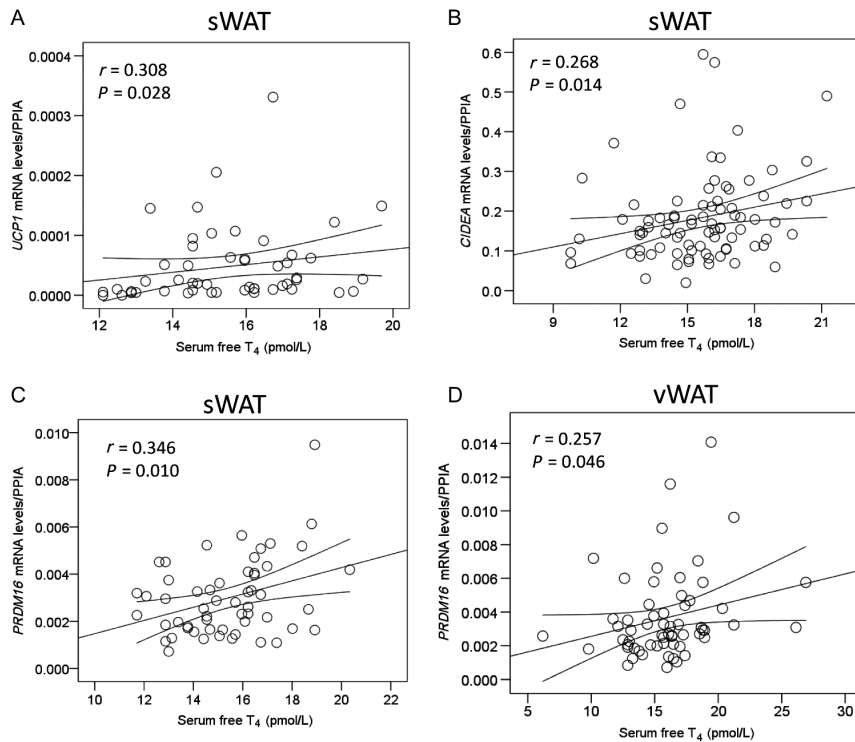
humans. The effect of THs is centrally mediated involving specifically the VMH, a key nucleus modulating energy balance (Morrison *et al.* 2014, Contreras *et al.* 2015, Lopez *et al.* 2016). Notably, this hypothalamic mechanism is mediated through AMPK, which has been described as a key factor regulating the actions of THs at the central level (Lopez *et al.* 2010, 2016, Alvarez-Crespo *et al.* 2016).

It has been known for more than a century that THs increase the basal metabolic rate (Magnus-Levy 1895). Typically, most of these effects have been related to the direct actions of THs on metabolically active tissues, such as the liver (Yen 2001), BAT (Bianco *et al.* 2005, Lopez *et al.* 2010, Ribeiro *et al.* 2010, Alvarez-Crespo *et al.* 2016), heart (Klein & Ojamaa 2001, Kahaly & Dillmann 2005) and skeletal muscle (Short *et al.* 2001). In those tissues, THs increase metabolic rate and thermogenesis by promoting the generation of energy and also by reducing the thermodynamic efficiency, which lead to heat production and increased temperature (Hulbert & Else 1981, Silva 2006, Lopez *et al.* 2013).

The process in which precursor cells placed in WAT become beige/brite cells, instead of white adipocytes,

**Figure 4**

Effect of AMPK overexpression in the VMH and central T<sub>3</sub> administration on WAT browning. (A) Bilateral GFP fluorescence in VMH (4×, scale bar 100 μm), (B) body weight change, (C) daily food intake, (D) representative H&E staining (left panels; 20×, scale bar: 100 μm) and adipocyte area (right panels), and (E) representative immunohistochemistry with anti-UCP1 antibody showing UCP1 staining (left panels; 20×, scale bar: 100 μm), UCP1-stained area (right panels) in gWAT of rats stereotaxically treated with GFP or AMPK $\alpha$ -CA adenovirus and ICV treated with vehicle or T<sub>3</sub>. Statistical significance was determined by ANOVA. *N* = 8 (only for the IHC analyses)-10 animals per group. Error bars represent s.e.m. \*\* and \*\*\**P* < 0.01 and 0.001 vs vehicle ICV GFP; #, ## and ###*P* < 0.05, 0.01 and 0.001 vs T<sub>3</sub> ICV GFP.

**Figure 5**

Correlation between T<sub>4</sub> circulating levels and browning markers in human WAT. Correlation between UCP1 (A), CIDEA (B) and PRDM16 (C) in sWAT and PRDM16 in vWAT (D) in human subjects.

is called browning (Fisher *et al.* 2012, Shabalina *et al.* 2013). Consequently, certain WAT depots significantly increase gene expression for UCP1 and their thermogenic capacity (Shabalina *et al.* 2013). Although the sWAT from the inguinal area is the most classical fat pad where browning studies have been performed, it has also been described in other depots, such as gonadal (Plum *et al.* 2007, Tews *et al.* 2013, Neinast *et al.* 2015, Contreras *et al.* 2016a, Fulzele *et al.* 2016, Jia *et al.* 2016, Lee *et al.* 2016, Martins *et al.* 2016, Shao *et al.* 2016). In this sense, it has been recently demonstrated that when centrally induced, browning affects gWAT in a similar extent to inguinal sWAT (Contreras *et al.* 2016a, Martins *et al.* 2016). However, despite the main thermogenic role of central THs, whether they are able to modulate the browning of WAT remains unclear. Here, we show that hyperthyroidism induces browning of WAT (sWAT from the inguinal area and gWAT) in rats. In our hyperthyroid model, T<sub>4</sub> was administered peripherally, which might imply the existence of direct effects of THs on white adipocytes, known to express TRs (Brent 2012, Lopez *et al.* 2013). Alternatively, THs may exert a central action after crossing the blood–brain barrier (BBB), which would be in agreement with recent evidence from our group, demonstrating that the metabolic effects of THs on brown fat are centrally mediated (Lopez *et al.* 2010, Alvarez-Crespo *et al.* 2016). Therefore, we investigated the

contribution of the central effects of THs on browning of WAT. Our data show that, when administered centrally, T<sub>3</sub> promotes a similar pattern of browning of WAT as observed in the hyperthyroid model. Remarkably, the central action of T<sub>3</sub> targets one particular hypothalamic nucleus, the VMH. Indeed, stereotaxic administration of the hormone into the ARC (a neighboring nucleus) did not recapitulate the effects on the browning program induced by T<sub>3</sub> within the VMH. Considering that the VMH also plays a major role in the modulation of BAT function via THs (Lopez *et al.* 2010, 2013, 2016, Alvarez-Crespo *et al.* 2016), our data suggest that this hypothalamic site is a key modulator of both white and brown fat activity.

Current evidence has demonstrated that inhibition of AMPK in the VMH plays a major role in mediating either the actions of THs on BAT (Lopez *et al.* 2010, 2013, 2016, Alvarez-Crespo *et al.* 2016) or the browning of WAT, for example by glucagon-like peptide 1 (GLP-1) agonism (Beiroa *et al.* 2014). To elucidate the contribution of hypothalamic AMPK activity on the browning of WAT by THs, we genetically activated AMPK in the VMH of rats centrally treated with T<sub>3</sub>. Our data showed that activation of AMPK totally blunted the effects of T<sub>3</sub> on WAT browning. Interestingly, this action was associated with a feeding-independent recovery of body mass, which was reduced by central T<sub>3</sub>. This evidence suggests that the augmented thermogenic capacity of brite adipocytes

**Table 2** Multivariate regression analyses to predict sWAT *CIDEA*, *PRDM16* and *UCP1* and vWAT *PRDM16* gene expression in the human cohort.

|                                    | sWAT <i>CIDEA</i> |             | sWAT <i>PRDM16</i> |             | sWAT <i>UCP1</i> |             | vWAT <i>PRDM16</i> |             |
|------------------------------------|-------------------|-------------|--------------------|-------------|------------------|-------------|--------------------|-------------|
|                                    | $\beta$           | <i>P</i>    | $\beta$            | <i>P</i>    | $\beta$          | <i>P</i>    | $\beta$            | <i>P</i>    |
| Age (years)                        | -0.16             | 0.15        | -0.14              | 0.28        | 0.08             | 0.6         | 0.15               | 0.25        |
| Sex                                | -0.05             | 0.63        | -0.01              | 0.92        | 0.14             | 0.38        | -0.12              | 0.34        |
| BMI (kg/m <sup>2</sup> )           | -0.21             | <b>0.04</b> | -0.17              | 0.19        | 0.05             | 0.76        | -0.27              | <b>0.03</b> |
| Serum free T <sub>4</sub> (pmol/L) | 0.24              | <b>0.03</b> | 0.35               | <b>0.01</b> | 0.4              | <b>0.02</b> | 0.24               | 0.05        |
| Adjusted R <sup>2</sup>            | 0.096 (9.6%)      |             | 0.105 (10.5%)      |             | 0.087 (8.7%)     |             | 0.101 (10.1%)      |             |
| <i>P</i> (model)                   | <b>0.018</b>      |             | <b>0.04</b>        |             | 0.1              |             | <b>0.04</b>        |             |

$\beta$  corresponds to the standardized beta coefficient of the multiple regression analyses. Bold indicates statistical significance.

(Shabalina *et al.* 2013) participates together with the BAT-mediated action in the weight-reducing effects of central T<sub>3</sub>.

Finally, we aimed to investigate whether browning markers correlate with circulating THs levels in humans. Remarkably, our results indicate that serum levels of T<sub>4</sub> are positively associated with *UCP1*, *CIDEA* and *PRDM16* in WAT. To our knowledge, this is the first demonstration that THs modulate WAT browning in humans. Whether increased WAT browning is observed in hyperthyroid patients is not reported, but considering that THs also stimulate BAT in humans (Lahesmaa *et al.* 2014) and that most of the human BAT is actually beige fat (Jespersen *et al.* 2013, Shinoda *et al.* 2015), it is tempting to speculate that browning of WAT may account for the increased energy expenditure that characterizes hyperthyroidism (Warner & Mittag 2012, Lopez *et al.* 2013). In this sense, we have performed some preliminary studies in hyperthyroid patients and detected a trend in the correlation between *UCP1* mRNA expression and T<sub>4</sub>; however, further work will be necessary to properly investigate this association. If that is the case, strategies to modulate browning might be of therapeutic benefit in controlling the effects of thyrotoxicosis. This latter possibility is particularly relevant in the context of life-threatening conditions, such as thyroid storm, for which current treatments are not satisfactory. In addition, the induction of browning by TR agonism might be a suitable strategy for the treatment of obesity. In this regard, recent data have shown that treatment with the TR agonist GC-1 promotes browning of WAT and ameliorates obesity and diabetes in mice (Lin *et al.* 2015).

In summary, our results make evident the importance of THs in the browning of WAT in rodent and humans. This observation provides new insights into the physiological effects of THs and also in the pathogenesis of hyperthyroidism-induced effects on energy balance; it

also suggests potential therapeutic strategies to counteract this disorder or other catabolic states.

#### Supplementary data

This is linked to the online version of the paper at <http://dx.doi.org/10.1530/JOE-16-0425>.

#### Declaration of interest

The authors declare that there is no conflict of interest that could be perceived as prejudicing the impartiality of the research reported.

#### Funding

The research leading to these results has received funding from the European Community's Seventh Framework Programme (FP7/2007–2013) under grant agreement n° 281854 – the *ObERStress* project (M L, Xunta de Galicia (R N: 2015-CP080 and PIE13/00024; M L: 2015-CP079), MINECO co-funded by FEDER (R N: BFU2015-70664-R; C D: BFU2014-55871-P; M L: SAF2015-71026-R and BFU2015-70454-REDT/*Adipoplast*). CIBER de Fisiopatología de la Obesidad y Nutrición is an initiative of ISCIII. The funders had no role in study design, data collection and analysis, decision to publish or in the preparation of the manuscript.

#### Author contribution statement

N M-S, J M M-N, C C and E R-P performed the *in vivo* experiments (hormonal, drug and viral treatments) and the analytical methods (real-time quantitative PCR and immunohistochemistry). N M-S, J M M-N, J F, R N, C D, J M F-R and M L designed the experiments, analyzed, discussed and interpreted the data. N M-S, J M M-N and M L made the figures. M L developed the hypothesis, coordinated and directed the project and wrote the manuscript. All authors reviewed and edited the manuscript and had final approval of the submitted manuscript.

#### Acknowledgements

The authors thank Patricia Seoane-Collazo and Ismael González-García (University of Santiago de Compostela) for their comments and criticisms.

#### References

Alvarez-Crespo M, Csikasz RI, Martinez-Sanchez N, Dieguez C, Cannon B, Nedergaard J & Lopez M 2016 Essential role of

- UCP1 modulating the central effects of thyroid hormones on energy balance. *Molecular Metabolism* **5** 271–282. (doi:10.1016/j.molmet.2016.01.008)
- Beiroa D, Imbernon M, Gallego R, Senra A, Herranz D, Villaroya F, Serrano M, Ferno J, Salvador J, Escalada J, et al. 2014 GLP-1 agonism stimulates brown adipose tissue thermogenesis and browning through hypothalamic AMPK. *Diabetes* **63** 3346–3358. (doi:10.2337/db14-0302)
- Bianco AC, Sheng XY & Silva JE 1988 Triiodothyronine amplifies norepinephrine stimulation of uncoupling protein gene transcription by a mechanism not requiring protein synthesis. *Journal of Biological Chemistry* **263** 18168–18175.
- Bianco AC, Maia AL, da Silva WS & Christoffolete MA 2005 Adaptive activation of thyroid hormone and energy expenditure. *Bioscience Reports* **25** 191–208. (doi:10.1007/s10540-005-2885-6)
- Brent GA 2012 Mechanisms of thyroid hormone action. *Journal of Clinical Investigation* **122** 3035–3043. (doi:10.1172/JCI60047)
- Brenta G, Danzi S & Klein I 2007 Potential therapeutic applications of thyroid hormone analogs. *Nature Clinical Practice Endocrinology and Metabolism* **3** 632–640. (doi:10.1038/ncpendmet0590)
- Cannon B & Nedergaard J 2004 Brown adipose tissue: function and physiological significance. *Physiological Reviews* **84** 277–359. (doi:10.1152/physrev.00015.2003)
- Cao L, Choi EY, Liu X, Martin A, Wang C, Xu X & Daring MJ 2011 White to brown fat phenotypic switch induced by genetic and environmental activation of a hypothalamic-adipocyte axis. *Cell Metabolism* **14** 324–338. (doi:10.1016/j.cmet.2011.06.020)
- Cohen P, Levy JD, Zhang Y, Frontini A, Kolodin DP, Svensson KJ, Lo JC, Zeng X, Ye L, Khandekar MJ, et al. 2014 Ablation of PRDM16 and beige adipose causes metabolic dysfunction and a subcutaneous to visceral fat switch. *Cell* **156** 304–316. (doi:10.1016/j.cell.2013.12.021)
- Contreras C, Gonzalez-Garcia J, Martinez-Sanchez N, Seoane-Collazo P, Jacas J, Morgan DA, Serra D, Gallego R, Gonzalez F, Casals N, et al. 2014 Central ceramide-induced hypothalamic lipotoxicity and ER stress regulate energy balance. *Cell Reports* **9** 366–377. (doi:10.1016/j.celrep.2014.08.057)
- Contreras C, Gonzalez F, Ferno J, Dieguez C, Rahmouni K, Nogueiras R & Lopez M 2015 The brain and brown fat. *Annals of Medicine* **47** 150–168. (doi:10.3109/07853890.2014.919727)
- Contreras C, Gonzalez-Garcia J, Seoane-Collazo P, Martinez-Sanchez N, Linares-Pose L, Rial-Pensado E, Ferno J, Tena-Sempere M, Casals N, Dieguez C, et al. 2016a Reduction of hypothalamic ER stress activates browning of white fat and ameliorates obesity. *Diabetes* **66** 87–99. (doi:10.2337/db15-1547)
- Contreras C, Nogueiras R, Dieguez C, Medina-Gomez G & Lopez M 2016b Hypothalamus and thermogenesis: Heating the BAT, browning the WAT. *Molecular and Cellular Endocrinology* **438** 107–115. (doi:10.1016/j.mce.2016.08.002)
- Cousin B, Cinti S, Morrioni M, Raimbault S, Ricquier D, Penicaud L & Casteilla L 1992 Occurrence of brown adipocytes in rat white adipose tissue: molecular and morphological characterization. *Journal of Cell Science* **103** 931–942.
- Fisher FM, Kleiner S, Douris N, Fox EC, Mepani RJ, Verdeguer F, Wu J, Kharitonov A, Flier JS, Maratos-Flier E, et al. 2012 FGF21 regulates PGC-1alpha and browning of white adipose tissues in adaptive thermogenesis. *Genes and Development* **26** 271–281. (doi:10.1101/gad.177857.111)
- Fulzele K, Lai F, Dedic C, Saini V, Uda Y, Shi C, Tuck P, Aronson JL, Liu X, Spatz JM, et al. 2016 Osteocyte-secreted Wnt signaling inhibitor sclerostin contributes to beige adipogenesis in peripheral fat depots. *Journal of Bone and Mineral Research* [in press]. (doi:10.1002/jbmr.3001)
- Gavaldà-Navarro A, Moreno-Navarrete JM, Quesada-Lopez T, Cairo M, Giralt M, Fernandez-Real JM & Villarroya F 2016 Lipopolysaccharide-binding protein is a negative regulator of adipose tissue browning in mice and humans. *Diabetologia* **59** 2208–2218. (doi:10.1007/s00125-016-4028-y)
- Ghorbani M, Claus TH & Himms-Hagen J 1997 Hypertrophy of brown adipocytes in brown and white adipose tissues and reversal of diet-induced obesity in rats treated with a beta3-adrenoceptor agonist. *Biochemical Pharmacology* **54** 121–131. (doi:10.1016/S0006-2952(97)00162-7)
- Gonzalez CR, Martinez de Morentin PB, Martinez-Sanchez N, Gomez-Diaz C, Lage R, Varela L, Dieguez C, Nogueiras R, Castano JP & Lopez M 2012 Hyperthyroidism differentially regulates neuropeptide S system in the rat brain. *Brain Research* **1450** 40–48. (doi:10.1016/j.brainres.2012.02.024)
- Hulbert AJ & Else PL 1981 Comparison of the ‘mammal machine’ and the ‘reptile machine’: energy use and thyroid activity. *American Journal of Physiology* **241** R350–R356.
- Imbernon M, Beiroa D, Vazquez MJ, Morgan DA, Veyrat-Durebex C, Porteiro B, Diaz-Arteaga A, Senra A, Busquets S, Velasquez DA, et al. 2013 Central melanin-concentrating hormone influences liver and adipose metabolism via specific hypothalamic nuclei and efferent autonomic/JNK1 pathways. *Gastroenterology* **144** 636–649. (doi:10.1053/j.gastro.2012.10.051)
- Jespersen NZ, Larsen TJ, Peijs L, Dagaard S, Homoe P, Loft A, de JJ, Mathur N, Cannon B, Nedergaard J, et al. 2013 A classical brown adipose tissue mRNA signature partly overlaps with brite in the supraclavicular region of adult humans. *Cell Metabolism* **17** 798–805. (doi:10.1016/j.cmet.2013.04.011)
- Jia R, Luo XQ, Wang G, Lin CX, Qiao H, Wang N, Yao T, Barclay JL, Whitehead JP, Luo X et al. 2016 Characterization of cold-induced remodelling reveals depot-specific differences across and within brown and white adipose tissues in mice. *Acta Physiologica* **217** 311–324. (doi:10.1111/apha.12688)
- Kahaly GJ & Dillmann WH 2005 Thyroid hormone action in the heart. *Endocrine Reviews* **26** 704–728. (doi:10.1210/er.2003-0033)
- Kaptein EM, Beale E & Chan LS 2009 Thyroid hormone therapy for obesity and nonthyroidal illnesses: a systematic review. *Journal of Clinical Endocrinology and Metabolism* **94** 3663–3675. (doi:10.1210/jc.2009-0899)
- Klein I & Ojamaa K 2001 Thyroid hormone and the cardiovascular system. *New England Journal of Medicine* **344** 501–509. (doi:10.1056/NEJM200102153440707)
- Lahesmaa M, Orava J, Schalin-Jantti C, Soinio M, Hannukainen JC, Noponen T, Kirjavainen A, Iida H, Kudomi N, Enerback S, et al. 2014 Hyperthyroidism increases brown fat metabolism in humans. *Journal of Clinical Endocrinology and Metabolism* **99** E28–E35. (doi:10.1210/jc.2013-2312)
- Lee YH, Kim SN, Kwon HJ, Maddipati KR & Granneman JG 2016 Adipogenic role of alternatively activated macrophages in beta-adrenergic remodeling of white adipose tissue. *American Journal of Physiology: Regulatory, Integrative and Comparative Physiology* **310** R55–R65. (doi:10.1152/ajpregu.00355.2015)
- Lin JZ, Martagon AJ, Cimini SL, Gonzalez DD, Tinkey DW, Biter A, Baxter JD, Webb P, Gustafsson JA, Hartig SM, et al. 2015 Pharmacological activation of thyroid hormone receptors elicits a functional conversion of white to brown fat. *Cell Reports* **13** 1528–1537. (doi:10.1016/j.celrep.2015.10.022)
- Loncar D, Bedrica L, Mayer J, Cannon B, Nedergaard J, Afzelius BA & Svajcar A 1986 The effect of intermittent cold treatment on the adipose tissue of the cat. Apparent transformation from white to brown adipose tissue. *Journal of Ultrastructure and Molecular Structure Research* **97** 119–129. (doi:10.1016/S0889-1605(86)80012-X)
- Lopez M, Lage R, Saha AK, Perez-Tilve D, Vazquez MJ, Varela L, Sangiao-Alvarellos S, Tovar S, Raghay K, Rodriguez-Cuenca S, et al. 2008 Hypothalamic fatty acid metabolism mediates the orexigenic action of ghrelin. *Cell Metabolism* **7** 389–399. (doi:10.1016/j.cmet.2008.03.006)

- Lopez M, Varela L, Vazquez MJ, Rodriguez-Cuenca S, Gonzalez CR, Velagapudi VR, Morgan DA, Schoenmakers E, Agassandian K, Lage R, *et al.* 2010 Hypothalamic AMPK and fatty acid metabolism mediate thyroid regulation of energy balance. *Nature Medicine* **16** 1001–1008. (doi:10.1038/nm.2207)
- Lopez M, Alvarez CV, Nogueiras R & Dieguez C 2013 Energy balance regulation by thyroid hormones at central level. *Trends in Molecular Medicine* **19** 418–427. (doi:10.1016/j.molmed.2013.04.004)
- Lopez M, Nogueiras R, Tena-Sempere M & Dieguez C 2016 Hypothalamic AMPK: a canonical regulator of whole-body energy balance. *Nature Reviews Endocrinology* **12** 421–432. (doi:10.1038/nrendo.2016.67)
- Magnus-Levy A 1895 Ueber den respiratorischen Gaswechsel unter Einfluss de Thyroidea sowie unter verschiedenen pathologische Zustand. *Berliner Klinische Wochenschrift* **32** 652.
- Martinez de Morentin PB, Whittle AJ, Ferno J, Nogueiras R, Dieguez C, Vidal-Puig A & Lopez M 2012 Nicotine induces negative energy balance through hypothalamic AMP-activated protein kinase. *Diabetes* **61** 807–817. (doi:10.2337/db11-1079)
- Martinez de Morentin PB, Gonzalez-Garcia I, Martins L, Lage R, Fernandez-Mallo D, Martinez-Sanchez N, Ruiz-Pino F, Liu J, Morgan DA, Pinilla L, *et al.* 2014 Estradiol regulates brown adipose tissue thermogenesis via hypothalamic AMPK. *Cell Metabolism* **20** 41–53. (doi:10.1016/j.cmet.2014.03.031)
- Martins L, Seoane-Collazo P, Contreras C, Gonzalez-Garcia I, Martinez-Sanchez N, Gonzalez F, Zalvide J, Gallego R, Dieguez C, Nogueiras R, *et al.* 2016 A functional link between AMPK and orexin mediates the effect of BMP8B on energy balance. *Cell Reports* **16** 2231–2242. (doi:10.1016/j.celrep.2016.07.045)
- Minokoshi Y, Alquier T, Furukawa N, Kim YB, Lee A, Xue B, Mu J, Fougelle F, Ferre P, Birnbaum MJ, *et al.* 2004 AMP-kinase regulates food intake by responding to hormonal and nutrient signals in the hypothalamus. *Nature* **428** 569–574. (doi:10.1038/nature02440)
- Morrison SF, Madden CJ & Tupone D 2014 Central neural regulation of brown adipose tissue thermogenesis and energy expenditure. *Cell Metabolism* **19** 741–756. (doi:10.1016/j.cmet.2014.02.007)
- Nedergaard J & Cannon B 2014 The browning of white adipose tissue: some burning issues. *Cell Metabolism* **20** 396–407. (doi:10.1016/j.cmet.2014.07.005)
- Nedergaard J, Dicker A & Cannon B 1997 The interaction between thyroid and brown-fat thermogenesis. Central or peripheral effects? *Annals of the New York Academy of Sciences* **813** 712–717. (doi:10.1111/j.1749-6632.1997.tb51772.x)
- Neinast MD, Frank AP, Zechner JF, Li Q, Vishvanath L, Palmer BF, Aguirre V, Gupta RK & Clegg DJ 2015 Activation of natriuretic peptides and the sympathetic nervous system following Roux-en-Y gastric bypass is associated with gonadal adipose tissues browning. *Molecular Metabolism* **4** 427–436. (doi:10.1016/j.molmet.2015.02.006)
- Ortega FJ, Mercader JM, Moreno-Navarrete JM, Nonell L, Puigdecant E, Rodriguez-Hermosa JJ, Rovira O, Xifra G, Guerra E, Moreno M, *et al.* 2015 Surgery-induced weight loss is associated with the down-regulation of genes targeted by microRNAs in adipose tissue. *Journal of Clinical Endocrinology and Metabolism* **100** E1467–E1476. (doi:10.1210/jc.2015-2357)
- Pearce EN 2012 Update in lipid alterations in subclinical hypothyroidism. *Journal of Clinical Endocrinology and Metabolism* **97** 326–333. (doi:10.1210/jc.2011-2532)
- Plum L, Rother E, Munzberg H, Wunderlich FT, Morgan DA, Hampel B, Shanabrough M, Janoschek R, Konner AC, Alber J, *et al.* 2007 Enhanced leptin-stimulated Pi3k activation in the CNS promotes white adipose tissue transdifferentiation. *Cell Metabolism* **6** 431–445. (doi:10.1016/j.cmet.2007.10.012)
- Ribeiro MO, Bianco SD, Kaneshige M, Schultz JJ, Cheng SY, Bianco AC & Brent GA 2010 Expression of uncoupling protein 1 in mouse brown adipose tissue is thyroid hormone receptor-beta isoform specific and required for adaptive thermogenesis. *Endocrinology* **151** 432–440. (doi:10.1210/en.2009-0667)
- Shabalina IG, Petrovic N, de Jong JM, Kalinovich AV, Cannon B & Nedergaard J 2013 UCP1 in brite/beige adipose tissue mitochondria is functionally thermogenic. *Cell Reports* **5** 1196–1203. (doi:10.1016/j.celrep.2013.10.044)
- Shao M, Ishibashi J, Kusminski CM, Wang QA, Hepler C, Vishvanath L, MacPherson KA, Spurgin SB, Sun K, Holland WL, *et al.* 2016 Zfp423 maintains white adipocyte identity through suppression of the beige cell thermogenic gene program. *Cell Metabolism* **23** 1167–1184. (doi:10.1016/j.cmet.2016.04.023)
- Shinoda K, Luijten IH, Hasegawa Y, Hong H, Sonne SB, Kim M, Xue R, Chondronikola M, Cypess AM, Tseng YH, *et al.* 2015 Genetic and functional characterization of clonally derived adult human brown adipocytes. *Nature Medicine* **21** 389–394. (doi:10.1038/nm.3819)
- Short KR, Nygren J, Barazzoni R, Levine J & Nair KS 2001 T(3) increases mitochondrial ATP production in oxidative muscle despite increased expression of UCP2 and -3. *American Journal of Physiology: Endocrinology and Metabolism* **280** E761–E769.
- Silva JE 2006 Thermogenic mechanisms and their hormonal regulation. *Physiological Reviews* **86** 435–464. (doi:10.1152/physrev.00009.2005)
- Tews D, Fischer-Posovszky P, Fromme T, Klingenspor M, Fischer J, Ruther U, Marienfeld R, Barth TF, Moller P, Debatin KM, *et al.* 2013 FTO deficiency induces UCP-1 expression and mitochondrial uncoupling in adipocytes. *Endocrinology* **154** 3141–3151. (doi:10.1210/en.2012-1873)
- Varela L, Martínez-Sánchez N, Gallego R, Vázquez MJ, Roa J, Gándara M, Schoenmakers E, Nogueiras R, Chatterjee K, Tena-Sempere M, *et al.* 2012 Hypothalamic mTOR pathway mediates thyroid hormone-induced hyperphagia in hyperthyroidism. *Journal of Pathology* **227** 209–222. (doi:10.1002/path.3984)
- Villarroya F & Vidal-Puig A 2013 Beyond the sympathetic tone: the new brown fat activators. *Cell Metabolism* **17** 638–643. (doi:10.1016/j.cmet.2013.02.020)
- von Ballmoos C, BC, Wiedenmann A & Dimroth P 2009 Essentials for ATP synthesis by F1F0 ATP synthases. *Annual Review of Biochemistry* **78** 649–672. (doi:10.1146/annurev.biochem.78.081307.104803)
- Warner A & Mittag J 2012 Thyroid hormone and the central control of homeostasis. *Journal of Molecular Endocrinology* **49** R29–R35. (doi:10.1530/JME-12-0068)
- Whittle AJ, Carobbio S, Martins L, Slawik M, Hondares E, Vazquez MJ, Morgan D, Csikasz RI, Gallego R, Rodriguez-Cuenca S, *et al.* 2012 BMP8B increases brown adipose tissue thermogenesis through both central and peripheral actions. *Cell* **149** 871–885. (doi:10.1016/j.cell.2012.02.066)
- Woods A, Azzout-Marniche D, Foretz M, Stein SC, Lemarchand P, Ferre P, Fougelle F & Carling D 2000 Characterization of the role of AMP-activated protein kinase in the regulation of glucose-activated gene expression using constitutively active and dominant negative forms of the kinase. *Molecular and Cellular Biology* **20** 6704–6711. (doi:10.1128/MCB.20.18.6704-6711.2000)
- Yen PM 2001 Physiological and molecular basis of thyroid hormone action. *Physiological Reviews* **81** 1097–1142.
- Yoneshiro T, Aita S, Matsushita M, Kayahara T, Kameya T, Kawai Y, Iwanaga T & Saito M 2013 Recruited brown adipose tissue as an antiobesity agent in humans. *Journal of Clinical Investigation* **123** 3404–3408. (doi:10.1172/JCI67803)

Received in final form 20 November 2016

Accepted 2 December 2016

Accepted Preprint published online 2 December 2016